Basic Characteristics of an Outer Rotor Consequent-pole Bearingless Drive

Tomohiro Yamada,
Akira Chiba
Department of Electrical Engineering
Tokyo University of Science
2641 Yamazaki Noda Chiba Japan
chiba@ee.noda.tus.ac.jp

Atsushi Nakajima,
Takeshi Hoshino
Institute of Aerospace Technology
Japan Aerospace Exploration Agency
7-44-1 Jindaiji-higashi-mati, Chofu-shi, Tokyo, Japan
nakajima@chofu.jaxa.jp

Tadashi Fukao,
Masatsugu Takemoto
Department of Mechanical Systems Engineering
Musashi Institute of Technology
1-28-1 Tamazutsumi Setagaya-ku, Tokyo, Japan
tfukao@me.musashi-tech.ac.jp

Masahide Oshima
Department of Electronic Systems Engineering
Tokyo University of Science, Suwa College
5000-1 Toyohira, Chino, Nagano, Japan
moshima@rs.suwa.tus.ac.jp

Osamu Ichikawa
Department of Mechanical and Control System Engineering
Polytechnic University
4-1-1 Hashimotodai, Sagamihara, Kanagawa, Japan
ichi@ieee.org

***Abstract* – An outer rotor consequent-pole bearingless drive is proposed with two-axis active position regulation having one unit of a bearingless motor. The other axis positions are supported by passive magnetic bearings. In this paper, basic characteristics are presented.**

***Index Terms* – bearingless motor; magnetic bearing; consequent-pole**

I. INTRODUCTION

In recent years, magnetically suspended drives are required for flywheel, pump and compressor drives. A bearingless drive consisting of an integrated motor with a magnetic bearing function has been actively developed [1]-[7]. Compact magnetically suspended bearingless drives are applicable for flywheel satellite posture regulation and home appliance energy storage system.

A consequent-pole bearingless motor drive with two radial axis positioning has been proposed by the authors [8]. For the remaining three-axis positioning, passive permanent magnet bearings are constructed. Three-dimensional analysis is carried out for force analysis. With the passive magnetic bearings, stiffness is enhanced in the three-axis movements, i.e., axial and conical directions. However, negative stiffness is resulted in the two radial axes. The bearingless motor is responsible for the cancellation of the negative stiffness.

In this paper, basic characteristics including three-dimensional analysis and experimental results are presented. A test drive is constructed by two-axis active position regulation having one unit of a bearingless motor with a consequent-pole PM rotor. Successful suspension and rotation of a rotor is presented.

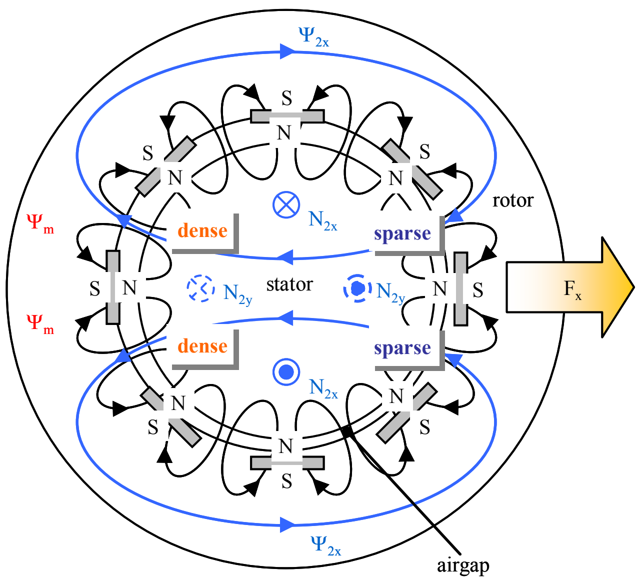

Fig.1 Principle of suspension force generation

II. PRINCIPLE OF SUSPENSION FORCE GENERATION IN CONSEQUENT-POLE BEARINGLESS MOTOR

Fig.1 shows a principle of suspension force generation in cross section of a consequent-pole bearingless motor. Stator iron core, windings and a shaft are constructed inside. On the outside, an outer rotor is constructed. At the inner surface of the rotor, eight permanent magnets are inset on the rotor iron. All the magnetizing directions of these permanent magnets are in the same direction, i.e., N-pole at the airgap between the rotor and stator. As all the permanent magnets are set N-pole inside, the iron parts between permanent magnets are consequently magnetized as S-pole. The arrowed circulars indicate the main fluxes Ψ_m of permanent magnet excitation. Two sets of three-phase windings are provided in the stator, one is for motor drive and another is for suspension. The motor drive winding sets are arranged in 16 poles because the rotor has eight permanent magnet poles and eight iron poles.

In the inner stator core, both motor and suspension windings are wound, although only suspension conductors are drawn. With a current in N_{2x} conductors, Ψ_{2x} fluxes are generated. These fluxes go into the iron parts of the rotor because magnetic reluctance is low. With the interaction of two fluxes Ψ_m and Ψ_{2x}, suspension force is generated in x-axis. Negative current in N_{2x} results in negative x-axis suspension force. Current in N_{2y} generates y-axis suspension force. The x- and y-axis conductors are composed of conventional three-phase two-pole windings. By the vector sum of these forces, suspension force can be generated in any desired directions.

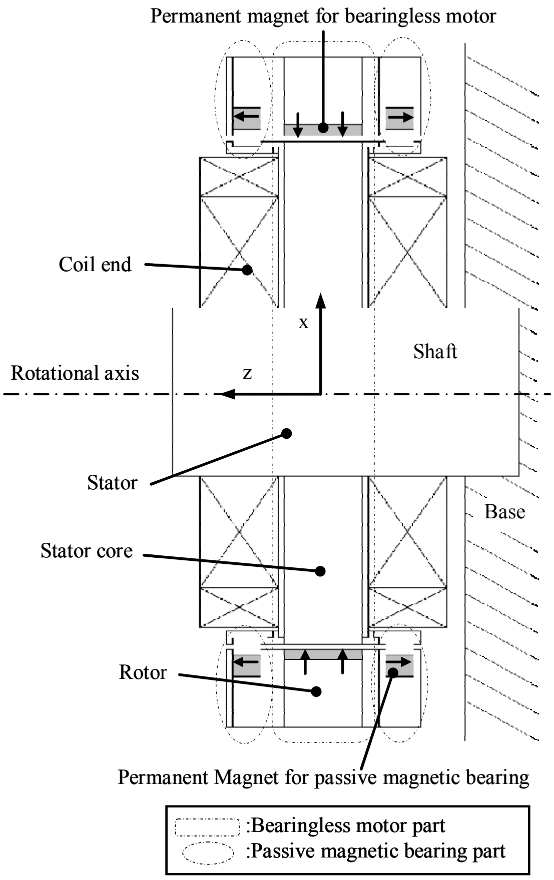

Fig.2 Structure of proposed drive

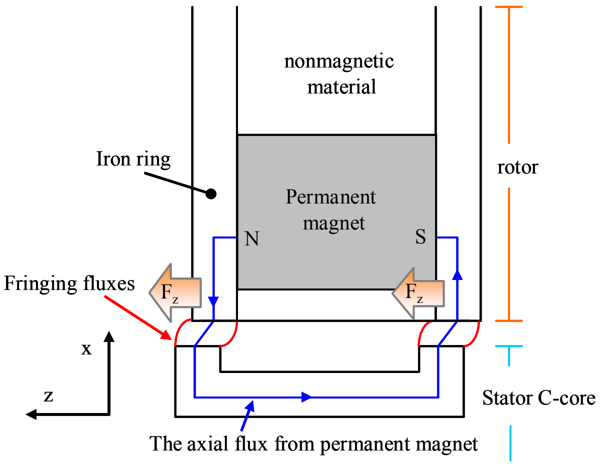

Fig.3 Passive magnetic bearings

III. Structure of Bearingless Motor and Passive Magnetic Bearings

Fig.2 shows the x-z cross section of the proposed bearingless motor drive. A rotating part is in ring shape surrounding the stator part. In the stator part, a shaft is fixed to a base. Around the shaft, a stator core and windings are constructed. In the rotor part, there are three permanent magnet layers. The center permanent magnets are radially magnetized, and are used for the bearingless motor functions generating torque and radial active forces. The rotor radial movements in x- and y- directions are detected by displacement sensors. The permanent magnets in the left and right are for axial-conical passive magnetic bearings. It is noted that the passive magnetic bearing is constructed around coil ends for the sake of compactness.

Fig.3 shows the enlarged cross section of the passive magnetic bearing part. The flux from a permanent magnet flows to a thin iron ring, an airgap, a confronting stator C-core and returns to the rotor permanent magnet. When the rotor is displaced in axial or conical directions, fringing fluxes in the airgap generate restoring force. As a result, the axial and conical movements are passively adjusted. It is noted that this passive magnetic bearing is unstable in radial directions. Thus, radial stable force should be provided by the actively controlled bearingless motor.

Fig.4 shows a schematic diagram of the control system. In the suspension controller, the radial positions are detected by displacement sensors and compared with the references. The PID controllers generate the current commands i^*_x and i^*_y. The 3-phase winding currents are detected by current sensors and transformed into 2-phase and compared with the current commands. The PI controllers generate the voltage commands V^*_x and V^*_y. Instantaneous 3-phase voltage commands are generated by a 2-phase-to-3-phase transformation, and the 3-phase inverter provides the 3-phase voltage for the suspension windings.

In the motor drive controller, from the speed command and the d- and q-axis current commands, 2-phase current commands are generated for 16-pole motor operation. Then the 3-phase winding currents are detected by current sensors and compared with the current commands. The PI controllers generate the voltage commands. Instantaneous 3-phase voltage commands are generated by a 2-phase-to-3-phase transformation, and the 3-phase inverter provides the 3-phase voltage for the motor drive windings.

IV. ANALYSIS RESULTS

Three-dimensional Finite Analysis is used for the static force analysis of the proposed bearingless motor. Magnetic bearing is cylindrical, in addition, radial force in a consequent-pole rotor is basically not depending on the rotor rotational position, thus, the rotor rotational position is fixed in the analysis. Fig.5 shows the analysis model of an outer rotor consequent-pole bearingless motor.

A. Radial unbalance force

Fig.6 shows the radial unbalance forces generated in the bearingless motor and passive magnetic bearing parts. The rotor is moved in radial direction x, while the current of suspension windings is set to zero. The magnetic pull force is generated by permanent magnets in both passive magnetic bearings and a bearingless motor. Note that the bearingless motor part generated significant magnetic pull force, because the airgap surface area is large. The radial unbalance forces are the unstable force. Thus, the unstable force must be cancelled with active bearingless radial force generation.

Fig.7 shows the radial stiffness as a function of radial displacement. The negative stiffness caused by passive magnetic bearings is rather low, because the axial thickness of passive magnetic bearings is minimized so that the radial unbalance force can be reduced. The design needed a compromise of increasing the axial restoring force. Use of the passive bearings results in approximately 50% increase in negative stiffness at small radial displacement. The negative stiffness must be cancelled with active bearingless radial force generation. As the increase is 50%, a proportional controller can be designed to have enough positive stiffness to cancel the negative stiffness.

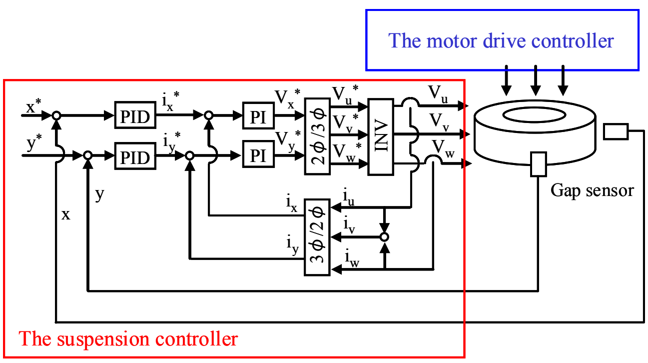

Fig.4 Schematic of control

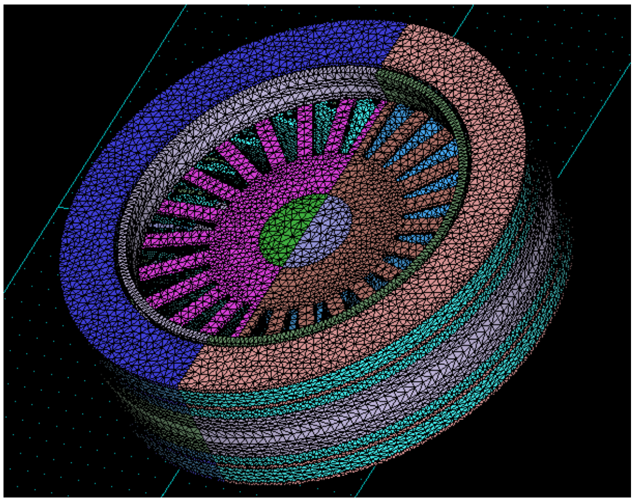

Fig.5 The analysis model

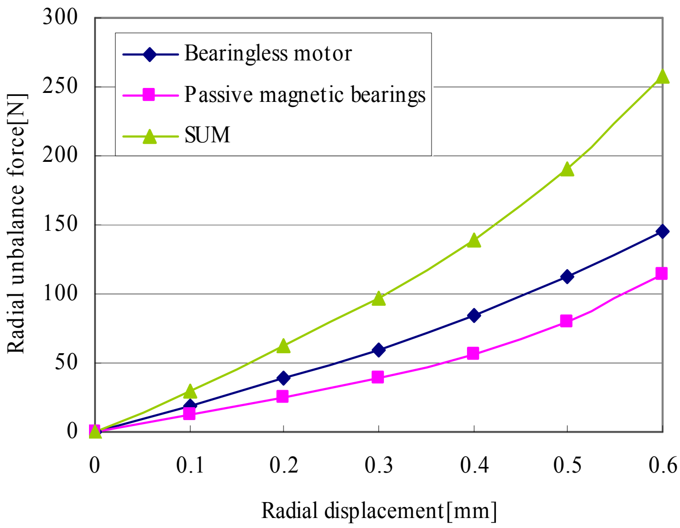

Fig.6 Radial unbalance force

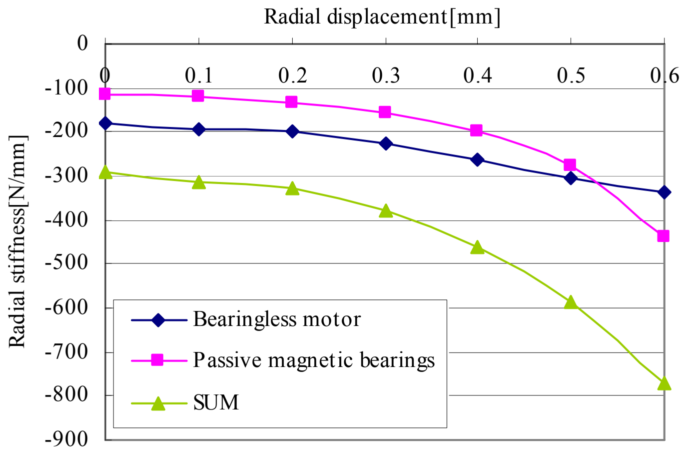

Fig.7 Radial stiffness

B. Radial suspension force

Fig.8 shows the radial suspension force in a bearingless motor part, while the rotor is positioned at the center. The rate of change of radial force is linear up to the current of 3 to 4A, i.e, about twice of the rated current, suspension force is saturated by magnetic saturation. The maximum radial force is about 130N. This value is rather low for consequent-pole bearingless motors, but the airgap flux density is designed to be rather low in this case to reduce iron loss. From Fig.6, the unbalance force of 130N is generated at the radial displacement of 0.35mm. Thus, the rotor radial movements should be limited to 0.35mm for a successful start in magnetic suspension.

C. Axial restoring force

Fig.9 shows the axial restoring forces generated in the bearingless motor part and the passive magnetic bearing parts. The restoring forces in Fig.9 are the function of axial rotor displacement. The axial restoring force of a passive magnetic bearing is high. Design optimization has been carried out to achieve high airgap flux density in the passive magnetic bearing part. Thick permanent magnets are used in the rotor with thin irons in the airgap. The iron part is designed to have less radial direction flux to minimize the unstable radial force.

Fig.10 shows the axial stiffness as a function of axial displacement. This is the derivative of restoring force. A positive stiffness is obtained in a wide range by the passive magnetic bearings. However, the stiffness of a bearingless motor becomes negative when the displacement is more than 0.8mm. At z=0, the sum of axial stiffness is effectively enhanced to 85N/mm. This value is about four times of 20N/mm in the case of a bearingless motor only.

D. Conical restoring torque

Fig.11 shows the conical restoring torque generated in the bearingless motor part and the passive magnetic bearing parts. The restoring torque in Fig.11 is the function of conical rotor displacement. The conical restoring torque of a passive magnetic bearing is high.

Fig.12 shows the conical stiffness as a function of conical displacement. This is a derivative of restoring torque with respect to rotational angle. A positive stiffness is obtained in a wide range by the passive magnetic bearings.

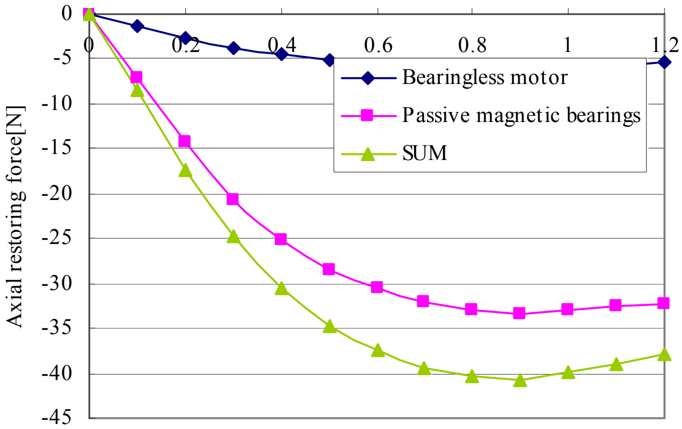

Fig.9 Axial restoring force

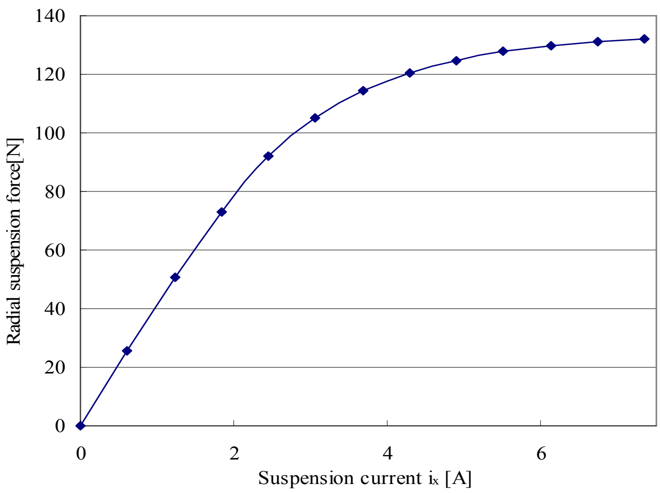

Fig.8 Radial suspension force

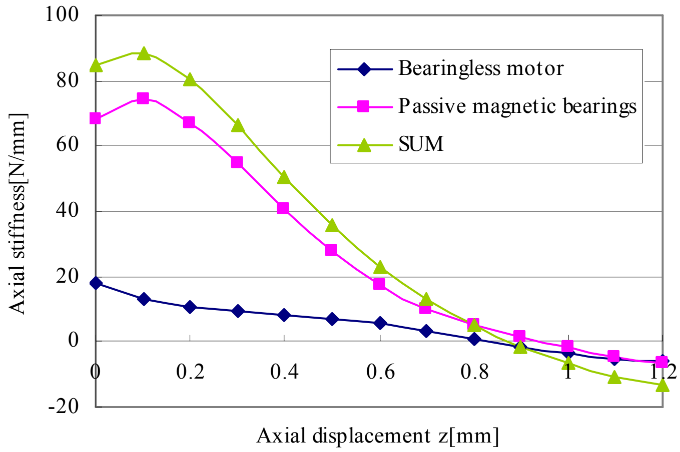

Fig.10 Axial stiffness

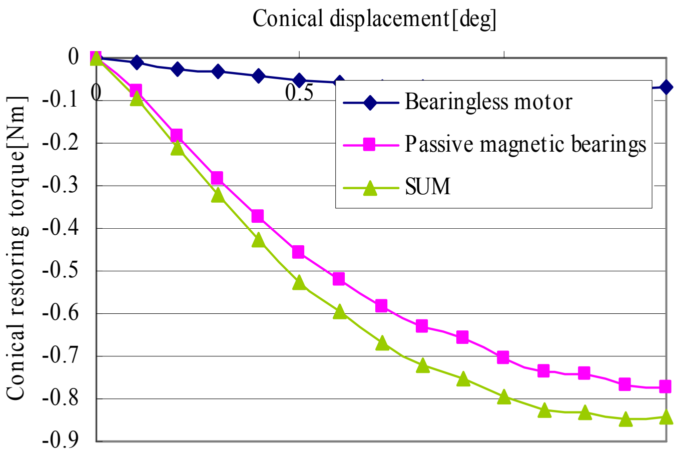

Fig.11 Conical restoring force

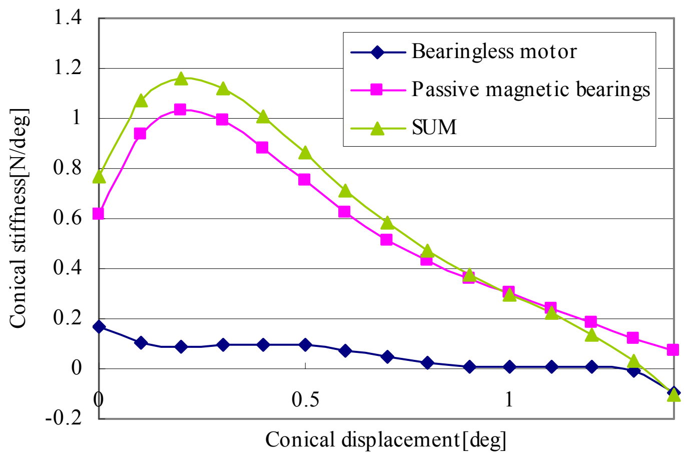

Fig.12 Conical stiffness

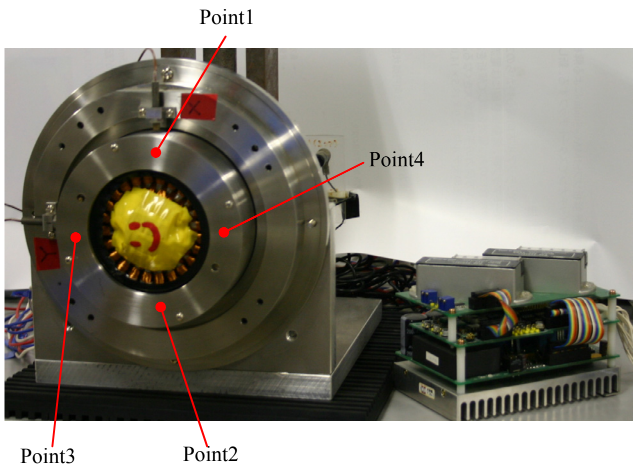

Fig.13 Picture of a test drive and controller

V. Experimental Results of a Test Drive

To confirm the proposed drive, a test drive was constructed and the suspension and rotation tests were performed. Fig.13 shows a picture of a test drive and controller. The front machine is an outer rotor consequent-pole bearingless motor. The controller is on the right side. The controller consists of the digital control system which was previously explained in detail in Fig.4, inverters and displacement sensor amplifiers. In experiment, the rotor radial displacements in x-y directions are detected. Axial-conical displacements in z direction are monitored by displacement sensors. The output voltages were observed by an oscilloscope.

A. Suspension test

During suspension test, the motor drive winding current was not provided. Before the suspension system is active, values of the rotor radial displacement in x-y directions are -500μm. The rotor was touched down. When the suspension system is activated the radial displacements quickly reduced.

Fig.14 shows the waveforms of current commands i^*_x, i^*_y and the rotor radial displacements in x-y directions in suspension test. A positive and negative step signal is added to displacement reference in y- direction while the rotor is suspended by magnetic force. The y-axis displacement follows the command. It is shown that the radial positions on the x-and y-axes are stably controlled.

Fig.15 shows the values of the rotor displacement in z direction, when the rotor was suspended. The rotor displacements in z direction were monitored at four points by displacement sensors. Fig.13 shows these points. At first, the rotor is pressed by a hand at the point between point1 and point4 while the rotor is suspended by magnetic force. Displacements of point1 and point4 are high, on the contrary displacements of point2 and point3 are low. It indicates that the rotor touches down in conical direction. The rotor is released at dotted line, displacements in z direction of the rotor converges. The values of the rotor axial-conical displacement were within touch down width, so the rotor is passively suspended in z, θ_x, and θ_y directions by the passive magnetic bearings.

B. Rotating test

During rotating test, the rotor was magnetically suspended. Fig.16 shows the waveforms of current commands i^*_x, i^*_y and the current waveform of the motor winding at 100r/min. Fig.17 shows the current waveforms of the motor winding and the rotor radial displacements in x-y directions at 100r/min. Note that the vibrations of the current commands i^*_x, and i^*_y occur in rotating test. But the rotor radial displacements in x-y directions are mostly zero. So it is shown that the radial positions on the x-and y-axes are stably controlled.

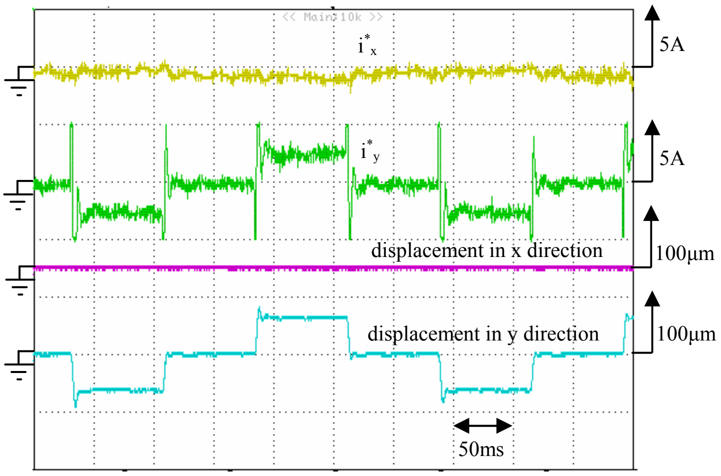

Fig.14 Suspension current commands and step radial displacements

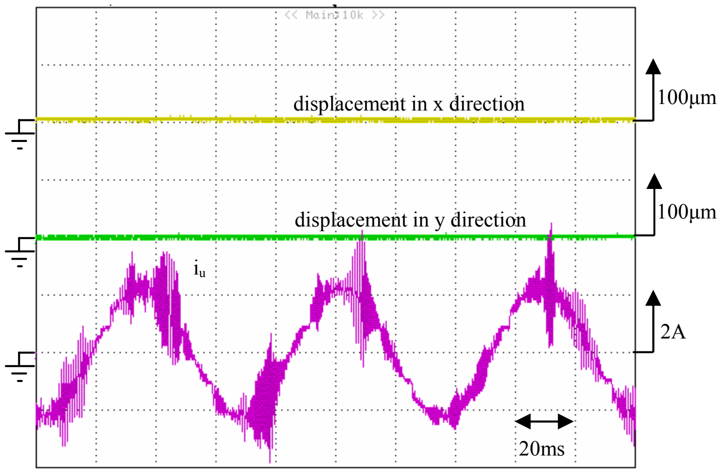

Fig.17 Radial displacements and motor current

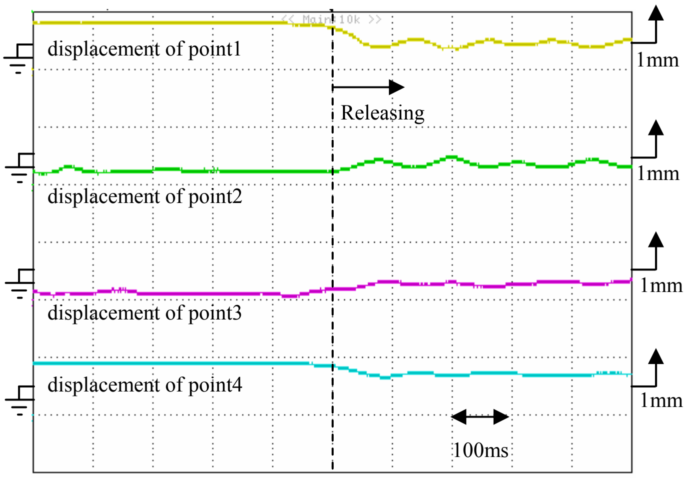

Fig.15 The axial-conical displacements

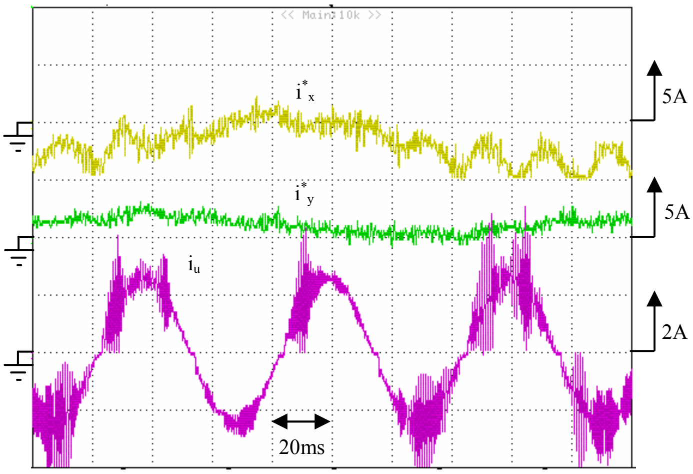

Fig.16 Suspension current commands and motor current

CONCLUSIONS

An outer rotor consequent-pole bearingless drive has been proposed. A test drive is constructed by two-axis active position regulation having one unit of a bearingless motor with a consequent-pole PM rotor. Successful suspension and rotation of a rotor is shown. Basic characteristics including three-dimensional analysis and experimental results are shown.

ACKNOWLEDGMENT

The authors would like to thank Mr. Kazuyoshi Asami who was a graduate student at the Tokyo University of Science.

REFERENCES

[1] Akira Chiba, Tadashi Fukao, Osamu Ichikawa, Masahide Oshima, Masatsugu Takemoto and David G. Dorrell "Magnetic Bearings and Bearingless Drives" Newnes Elsevier 2005 March 381pages ISBN 0 7506 5727 8

[2] K. Nenninger, W. Amrhein, S. Sillber, G. Trauner, and M. Reisinger, "Magnetic circuit design of a bearingless single-phase slice motor" in Proc. 8th Int. Symp. Magnetic Bearingless(ISMB), 2000, pp. 265-270

[3] H. Kanebako and Y. Okada, "New design of hybrid type self-bearing motor for high-speed miniature spindle" in Proc. 8th ISMB. Zurich, Germany, 2002, pp. 65-70

[4] M. Neff, N. Barletta, and R. Schob, "Bearingless centrifugal pump for highly pure chemicals" in Proc. 8th Int. Symp. Magnetic Bearing, 2002, pp. 283-288

[5] F. Wang and L. Xu "Calculation and measurement of radial and axial forces for a bearingless PMDC motor" in Proc. IEEE Industry Applications Conf.(IAS), vol.1, Rome, Italy, 2000, pp. 249-252

[6] Tomohiro Takenaga, Yutaka Kubota, Akira Chiba and Tadashi Fukao "A Principle and Winding Design of Consequent-pole Bearingless Motors" JSME International Journal Series C vol.46, no.2.June 2003 pp.363-369

[7] Jun Amemiya, Akira Chiba, David G Dorrell, Tadashi Fukao, "Basic Characteristics of a Consequent-Pole Type Bearingless Motor" IEEE Transaction on Magnetics January 2005 vol.41 no.1 pp.82-89

[8] Kazuyoshi Asami, Akira Chiba, Md. Azizur Rahman, Takeshi Hoshino, Atsushi Nakajima, "Stiffness Analysis of a Magnetically Suspended Bearingless Motor With Permanent Magnet Passive Positioning" IEEE Transaction on Magnetics, vol.41, no.10, pp.3820-3822,2005